

See discussions, stats, and author profiles for this publication at: <https://www.researchgate.net/publication/236954279>

Glacier hazard assessment in mountains using satellite optical data

Conference Paper · January 2005

CITATIONS

3

READS

174

8 authors, including:



Andreas Kääb

University of Oslo

278 PUBLICATIONS 12,605 CITATIONS

[SEE PROFILE](#)



Nadine Salzmann

Université de Fribourg

103 PUBLICATIONS 1,597 CITATIONS

[SEE PROFILE](#)



Jean F. Schneider

University of Natural Resources and Life Sciences Vienna

4 PUBLICATIONS 6 CITATIONS

[SEE PROFILE](#)

Some of the authors of this publication are also working on these related projects:



GlobPermafrost [View project](#)



Ambassadors Program at Planet [View project](#)

GLACIER HAZARD ASSESSMENT IN MOUNTAINS USING SATELLITE OPTICAL DATA

*Andreas Käab¹, Christian Huggel¹, Samuel Guex¹, Frank Paul¹, Nadine Salzmann¹,
Kostia Schmutz¹, Demian Schneider¹ and Yvo Weidmann²*

1. University of Zurich, Department of Geography, Zurich, Switzerland;
[kaeaeb\(at\)geo.unizh.ch](mailto:kaeaeb(at)geo.unizh.ch)
2. University of Applied Sciences, Muttenz, Basel, Switzerland

ABSTRACT

Process interactions and chain reactions, the shift of cryospheric hazard zones due to climate change, and the far reach of glacier disasters make it necessary to apply modern remote sensing techniques for the assessment of glacier hazards. In the present contribution we provide an overview of spaceborne optical methods suitable for glacial hazard assessment and disaster management. Digital terrain models (DTMs) represent one of the most important data sets for investigating high-mountain hazards. In the optical domain, DTMs are best derived from satellite along-track stereo from sensors such as ASTER or SPOT-5. Test studies suggest an accuracy of up to the pixel size of the applied sensor for conditions of good optical contrast and smooth topography. Fusion of such photogrammetrically derived DTMs with the DTM from the Shuttle Radar Topography Mission (SRTM) is a promising way to combine the advantages of both technologies and overcome some of the inherent problems. We demonstrate that large changes in terrain volume such as from avalanche deposits can indeed be measured by repeated satellite DTMs. Visual inspection and automatic classification based on repeated multispectral imagery is a well-developed tool for detecting potential hazard sources. Combination of such methods with DTMs significantly improves glacier hazard assessments. Multitemporal imagery can also be used to derive glacier movement, an important factor of glacier mass-balance and for the growth of ice-contact lakes.

Keywords: glacier, hazard, assessment, remote sensing.

INTRODUCTION

Glacial disasters can cause thousands of casualties in one event. Related damages or mitigation costs are on the order of several 100 million Euro as a long-term annual average global sum (1). Glacier hazards in high mountains include glacier-related floods, stable and unstable glacier length changes and glacier fluctuations, paraglacial mass movements, thermal, mechanic and hydrological impacts from changes in glacierisation, and hazards from glacier-clad volcanoes. Often, combinations of these (and other) processes lead to the most severe glacier catastrophes. Whilst above direct glacier hazards are very palpable, so too are indirect hazards, such as changes in dry-season river flows, adverse effects on mountain tourism, and related socio-economic consequences.

Assessment and management of glacial hazards requires the application of modern integrative earth-observation techniques for a number of reasons (1):

- Typically, related hazard source areas are situated in remote high-mountain regions, often difficult to access physically for topographic, political and/or security reasons (e.g. Caucasus, Colombia, Central Asia, Kashmir, etc.).
- The remote location of most glacial hazard sources, the potential process interactions and chain reactions, and the far reach of some of the high-mountain hazards require remote sensing sensors capable to cover large areas at once.
- Climate change induces disturbance in glacier and permafrost equilibrium and can shift hazard zones beyond historical knowledge. In addition, human settlements and activities increasingly

extend towards endangered zones in many regions. As a result, historical data alone are not sufficient any more for hazard assessments and have to be combined with new observation and modelling approaches.

- Due to the accelerated change of high-mountain environments, hazard assessments shall be undertaken routinely and regularly, combined with continuous monitoring. Remote sensing is particularly suited for both regular and rapid observation.

Recent developments in spaceborne remote sensing open up new possibilities for the assessment of natural hazards in general (2,3) and glacier-related hazards in particular (4,5,6). Remote sensing will therefore substantially gain importance for such works in the near future.

The main aim of this contribution is to provide an overview of available optical spaceborne remote sensing methods and potential applications for high-mountain hazard assessment.

METHOD OVERVIEW

The applicability of remote sensing for high-mountain hazard assessments is predominantly governed by the following factors:

- *The spatial resolution* of the sensor decides about the degree of detail that can be detected from the data. Often, fine resolution is required to assess important parameters of glacier- and permafrost hazards (e.g. discrimination of debris versus rock surface).
- *The temporal resolution* (i.e. revisit time) of the remote sensing system has to be in agreement with the rate of hazard development, or the changes observed.
- *The timing* of data acquisition has to be under control of the user, or to coincide with the user needs by chance. The probability for the latter increases with temporal resolution.
- *The section of the electromagnetic spectrum* used determines among others the surface parameters that are recorded at the sensor and the sensitivity of the sensor to weather and illumination conditions.
- *Stereo, interferometric or ranging capability* of the remote sensing system enables the computation of terrain elevations.
- *Usability of data* for the user, with respect to e.g. existence of and access to data archives, speed of on-demand acquisition, speed of delivery, simplicity of data formats and size, financial resources of the user, hard- and software resources of the user, and processing and analysis knowledge of the user.

Beside many advantages of airborne remote sensing such as level of detail and comparably direct user control, this class of platforms is often not applicable for areas where topographic, political, security, or financial restrictions are involved. Satellite sensors overcome these restrictions in parts. They are able to cover large areas for mountain hazard assessments without ground access needed, data are comparably cheap and well accessible, and for some sensors a repeat cycle of a few days is possible.

Spaceborne optical remote sensing technologies for high-mountain hazard assessments (4,5,7):

- Optical multispectral spaceborne imaging represents a well-established satellite remote sensing method for mapping and monitoring ground cover and its changes. It is often used for detecting hazard source areas and terrain changes, and for mapping of endangered zones (8,9,10,11,12,13,14).
- Satellite optical stereo, usually combined with multispectral imaging, enables the computation of DTMs, an important prerequisite for most high-mountain studies (4,15,16).

Here, we do not cover microwave, and airborne and terrestrial remote sensing methods for glacial hazard assessment.

Image classification

The most common application of remotely sensed image data for high-mountain hazard assessment consists in the interpretation and classification of the image content. Thereby, both the spectral image information and its spatial context are exploited. In particular under conditions of difficult topographic conditions and low optical contrast, or for highly complex assessment tasks, manual image segmentation might be superior to semiautomatic and automatic techniques. However, for rapid, repeat, and/or large-area quantitative applications, automatic image classification is able to offer valuable support. The large variety of available techniques ranges from mono-spectral (i.e. grey-value) segmentations, multi- and hyperspectral classifications, to spatio-spectral analyses utilising not only the spectral information of the image pixels but also their spatial context (4).

For instance, glacierized areas (9,17,18,19,20,21,22,23) or glacier lakes (10,24) can be mapped automatically. Archived data sets are an invaluable source for comparison between past and present situations (11). For instance, a number of ASTER data before and after the 20 September 2002 Kolka-Karmadon rock-ice avalanche enabled mapping and better understanding of this disaster (Figure 1) (12). During this event, a rock-ice avalanche of several million m³ from the north face of the Kazbek massif sheared off the entire Kolka glacier tongue. The combined avalanche rushed down the Genaldon valley for 18 km, reaching speeds of up to 300 km h⁻¹. Approximately 100 million m³ of ice and debris were deposited at the village of Karmadon where the avalanche was stopped by a narrow gorge. Subsequently, a devastating mudflow was released, propagating down further 15 km (12,25,26,27).

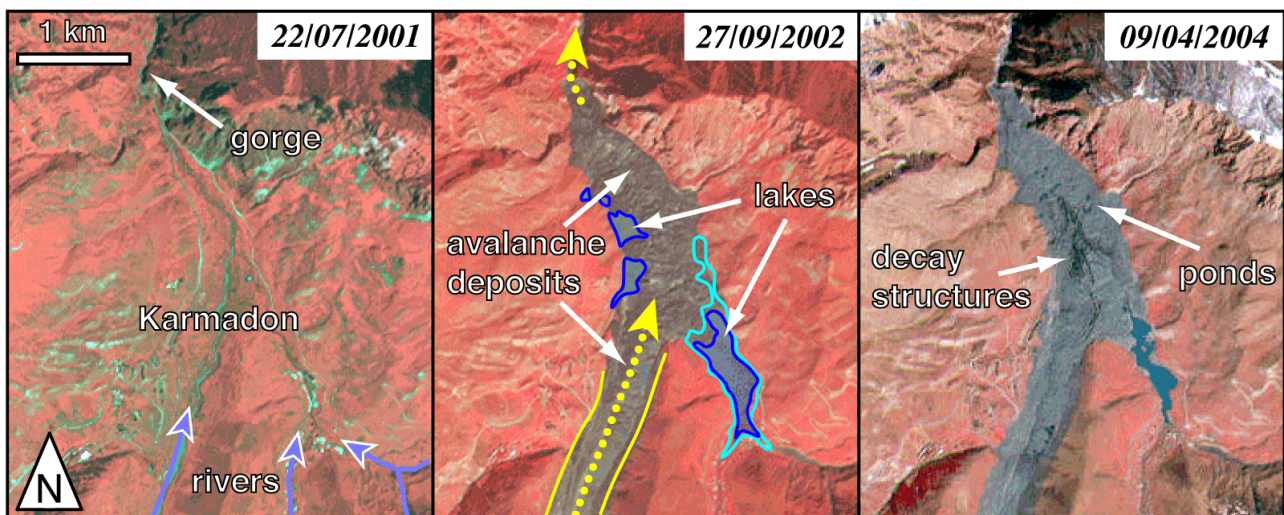


Figure 1: ASTER false color imagery of the Karmadon area from before (left) and after (middle and right) the 20/09/2002 Kolka/Karmadon rock-ice avalanche disaster, North Ossetia, Caucasus. The rivers in the area (blue arrows) were dammed by the avalanche deposits and formed lakes (dark blue line: lake extent as of 27/09/2002; light blue line: lake extent as of 22/10/2002). On the 09/04/2004 image, the rock-ice dam showed already distinct melt and decay structures.

Many glacier-related hazards are linked to terrain dynamics. Thus, multitemporal applications are of particular interest for assessing high-mountain hazards. Besides measuring elevation changes and terrain displacements discussed in the following sections, a group of change detection techniques is applied. Related strategies include (3,4,28,29)

- *multitemporal data overlay and comparison*, where the results from monotemporal image classifications are superimposed (e.g. lakes in Figure 1, middle panel)
- *animation*, where repeat images or derived classifications are shown sequentially (so-called "flickering") (29)
- *multitemporal false colour composites* (FCC), where the individual channels of a colour image (e.g. red, green, blue) are composed by images of different acquisition times (Figure 2) (4)

- *image algebra*, where a change image is computed from two or more multitemporal input images through algebraic band operations such as band ratios or normalised differences (4,28,30)
- *multitemporal principle component transformation (PCT)*, where the first principle component(s) computed from a multitemporal image data set tend to indicate the largest radiometric changes between the images (28). Multitemporal PCT can be useful for sets of many repeat data where FCCs or simple image algebra fail, e.g. for data from low-resolution sensors such as MODIS or MERIS, or for long time-series such as from the Landsat satellites.
- *multitemporal classifications*, where repeated data sets are included in a classification scheme and the "change classes" (e.g. ice-to-rock, debris-to-vegetated, ice-to-water) are derived automatically or through training areas.

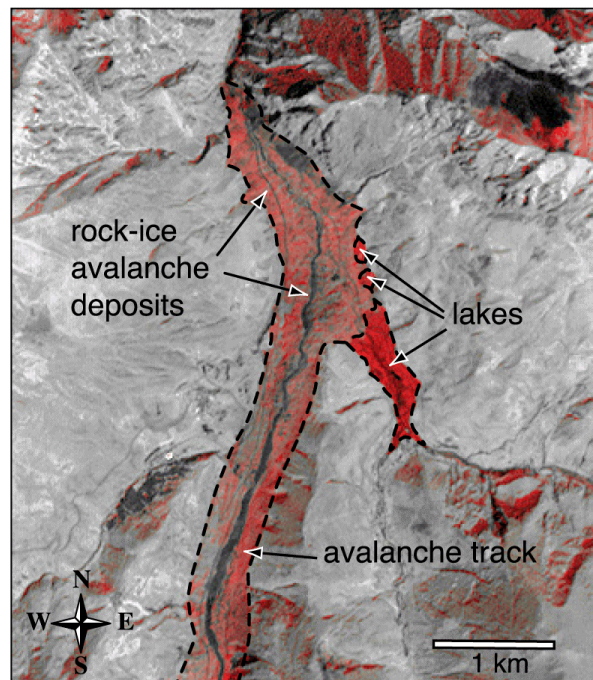


Figure 2: Deposits of the Kolka/Karmadon rock-ice avalanche (see Figure 1). Change detection is done by a multitemporal RGB-composite. Red: ASTER band 3 of 22/07/2001; Green and Blue: ASTER band 3 of 13/10/2002. Avalanche track and deposits, as well as lakes dammed by these deposits become visible in the false colour composite. The dashed outline marks the avalanche path running from south to north, the deposits in front of the Karmadon gorge at the upper edge of the image, and the lakes, which were dammed by the avalanche deposits. Red-coloured changes in northern slopes are due to different shadow/illumination conditions between the acquisition dates.

Particularly promising for hazard assessment and disaster management is the (multitemporal) fusion of optical and SAR data, because it is able to combine the advantages of different sections of the electromagnetic spectrum (3). In that way, for instance, SAR data can bridge gaps in optical time series due to cloud cover or snow humidity conditions that are hardly detectable from optical sensors and can be inferred from SAR into optical-based snow mapping (31,32,33).

Accurate co-registration of the repeat data, i.e. identical ground co-ordinates for identical (stable) terrain points, is a crucial prerequisite of any image change detection.

Digital terrain models from satellite stereo

DTMs represent one of the most important prerequisites for investigating high-mountain hazards, because many high-mountain geomorphic processes are driven by the relief energy. An efficient spaceborne way to generate such DTMs for nearly any place on the Earth is satellite along-track stereo from sensors such as ASTER or SPOT-5. For mountain environments with rapidly changing surface conditions such as snow cover, along-track stereo (acquired within minutes during one

overflight) is preferable to cross-track stereo that utilises imagery from neighbouring tracks, sometimes with a temporal baseline of weeks or months. Through digital photogrammetric methods DTMs can be produced for mountain terrain with a vertical accuracy approaching the pixel size of the applied sensor (e.g. 15 m for ASTER; Figure 3) and with typical horizontal grid spacings of 2-4 pixel in size (19,30,34,35,36,37).

Large errors, however, can occur

- on steep flanks facing away from the oblique stereo sensor (e.g., for the descending ASTER orbit northern slopes are strongly distorted or even hidden in the back-looking stereo channel),
- for particularly rough topography with sharp peaks, that are too small to be clearly identified in both stereo partners, and
- for insufficient optical contrast (e.g. snow cover).

In such cases, the stereo parallaxes required for DTM generation can be matched at different image resolutions and/or using different image chip sizes. Coarser image resolutions and larger matching chip sizes tend to produce more robust but less detailed DTMs. Potential DTM errors can then be detected from analysing the vertical deviations between the different DTMs (30,38,39,40). Further, filters are available in order to detect and eliminate sharp spikes and holes in DTMs (38).

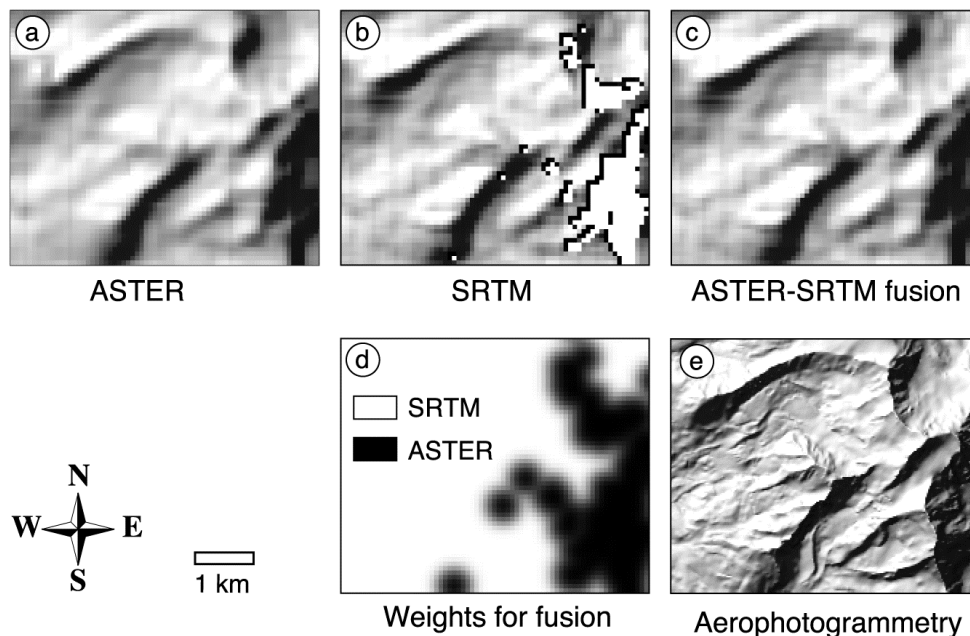


Figure 3: Fusion between a DTM from ASTER stereo and SRTM. (a) hillshade of an ASTER DTM of the Gruben area, Swiss Alps, derived at 60 m resolution; (b) SRTM DTM with data gaps in white; (c) fusion between both DTMs; (d) fusion weights for filling the SRTM gaps with ASTER DTM data (white: SRTM is used, black: ASTER is used; grey: weight of SRTM elevation values with respect to ASTER DTM); (e) aerophotogrammetric DTM for comparison.

Often, DTM errors are accompanied by low correlation values from the stereo-parallax matching procedure between the stereo image partners and can thus be detected using the so-called matching score-channel of the DTM (40). The procedure can be combined with the above multi-level error detection.

A further simple and efficient method for evaluating DTMs and detecting severe errors is to produce multiple orthoimages using the same DTM but source images from different positions (multi incidence-angle images) such as the stereo partners from along-track stereo. Thereby, vertical DTM errors translate into horizontal distortions, which become different for different incidence angles and can thus be easily visualised by animated overlay or other change detection techniques between the multi incidence-angle orthoimages (4,30,41).

DTMs from satellite stereo show characteristics such as data gaps, accuracy, etc., that are in parts different from the characteristics of InSAR-derived DTMs. It can, therefore, be of particular interest to merge DTMs from satellite stereo with DTMs from satellite InSAR, namely the SRTM DTM, in order to combine the advantages of both sensor types. Such DTM-fusion helps especially in finding severe vertical and horizontal DTM errors, and filling data gaps in either of the DTMs to be fused. DTM-merging techniques range from replacement of data (30,42), weighted fusion resulting in smooth transitions between DTMs (Figure 3) (40), to merging in support of the DTM processing (e.g. DTM-approximation to geometrically constrain stereo parallax matching or interferometric phase unwrapping) (43).

An important processing step before merging or comparing multi-source DTMs is to ensure accurate co-registration of the multiple data sets (for more details see below section on elevation changes).

TERRAIN ELEVATION CHANGES (DTM DIFFERENCES)

Terrain elevation changes over time, i.e. vertical differences between repeat DTMs, are indicators for geomorphodynamic processes such as glacier fluctuations and mass movements. Thus, their detection can be an important step of high-mountain hazard assessment and disaster mapping (44,45).

In general, changes in terrain elevation are derived by subtracting repeat DTMs. The accuracy of such derived vertical changes is, in principle, on the order of the accuracy of the repeat DTMs that are used. Special pre- and post-processing procedures help to reach or improve the latter accuracy:

Pre-processing, i.e. procedures beforehand the DTM subtraction: As for all multitemporal analyses, accurate co-registration of the multiple DTMs is a necessary prerequisite to obtain elevation changes free of systematic errors. If the repeat DTMs are produced using the same method (e.g. optical stereo), the co-registration of the DTMs (and other products) can be assured by orienting the original data as one common, multitemporal data set. Repeat satellite imagery should be oriented as one (multitemporal) image block with common ground control points (GCPs) and all the images connected by (multitemporal) tie points (30,39,46). If the original sensor model and orientation is inaccessible, or the DTMs have different sources, matching between the individual DTMs to be compared is recommended. For instance, through cross-correlation techniques the vertical and horizontal shifts of selected sections of the "slave" DTM with respect to the "master" DTM can be measured so that the vertical differences between the DTMs to be co-registered become minimal. From these shift vectors (Figure 4) an optimal horizontal and vertical shift, rotation, scale, etc., between the DTMs to be compared can be computed and the "slave" DTM be transformed accordingly (40). The section-wise DTM-to-DTM matching has to focus on stable terrain with sufficient relief (i.e. topographic contrast). Alternatively, also products using the DTMs can be matched, for instance orthoimages (36), or DTM derivatives such as slope or curvature maps, or edge-filtered DTMs. Thereby, the error propagation from the DTMs into the product to be matched has to be considered.

Post-processing of the elevation differences: Once the raw differences between repeat DTMs are computed it is often necessary to filter the elevation differences obtained, because the noise in the derived differences is larger than in the original DTMs (4). The task is to define a noise model adapted to the nature of the process under investigation. In general, low-pass filters exist for the spatial domain (e.g. median, medium, Gauss, etc.) or for the spectral domain (e.g. Fourier or wavelet) (4,47,48).

Compared to airborne techniques, elevation changes from repeat satellite stereo can only be measured for a limited number of geomorphodynamic processes due to the reduced accuracy of according DTMs. Nevertheless, the accuracy obtained might be good enough to detect and quantify large changes in terrain geometry, such as avalanche deposits or glacier mass changes (Figure 5) (4,36).

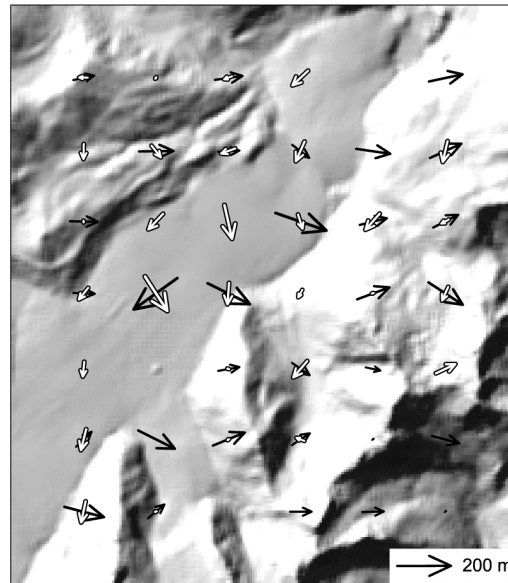


Figure 4: Horizontal residuals from matching the SRTM DTM (white arrows) and an ASTER DTM (black arrows) onto an aerophotogrammetric reference DTM. Glaciar Chico, Southern Patagonia Icefield, Chile. Matching grid width used was 1500 m, matching chip size was 750 m. For the flat glacier obvious mismatches occur due to missing topographic contrast. No residual vectors are available for the SRTM DTM in the lower right section due to data gaps. For the DTMs shifted according to the residual vectors the vertical deviations from the aerophotogrammetric DTM were reduced by about 10%.

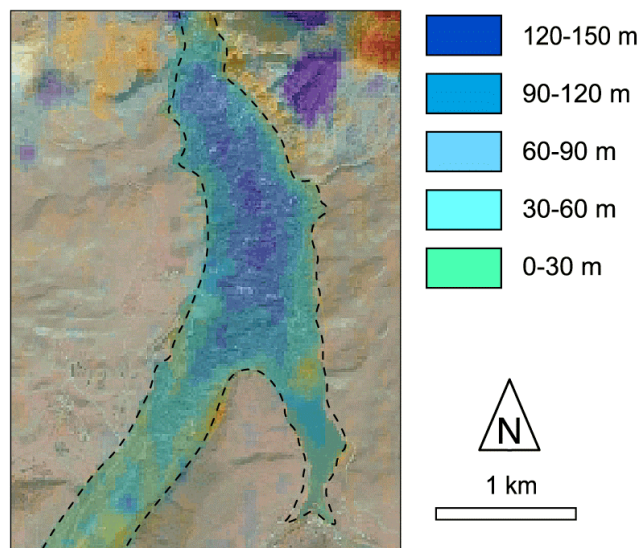


Figure 5: Thickness of the 20/09/2002 avalanche deposits at Karmadon (see Figure 1) computed from ASTER DTMs of 22/07/2001 and 06/10/2002. Background: ASTER orthoimage of 06/10/2002. The strong elevation changes to the upper right corner are due to errors in the ASTER DTM in steep slopes.

SURFACE DISPLACEMENTS

Terrain movements can directly pose a potential hazard (e.g. landslides) or provoke follow-up processes, which then represent or develop into hazards (e.g. river damming by a glacier surge). The measurement of terrain displacements from repeat image data can thus support high-mountain hazard assessments (49,50). If digital image correlation techniques are applied, the measurements are possible at a horizontal accuracy on the order of the pixel size of the sensor

applied. Sub-pixel accuracy can be reached as well but is often limited by changes in terrain and illumination conditions between the repeated data acquisitions. Image matching techniques can be applied equally to terrestrial photos, air photos, optical satellite images, SAR images (51,52), or high-resolution DTMs e.g. derived from laserscanning or aerophotogrammetry (4). Depending on the data and technique employed either the horizontal component of the surface displacement is measured or the fully three-dimensional surface displacement vector.

The rate of terrain movement, which can be detected at a statistically significant level of accuracy, depends among others on the image pixel size, the temporal baseline, and the terrain preservation between the repeated data acquisitions. From air and high-resolution satellite images (e.g. IKONOS, QuickBird, Orbview, SPOT-5) slow slope instabilities such as paraglacial rock mass movements or permafrost creep can be detected (i.e. movement rates in the order of cm to m per year) (49, 50). Comparably fast movements (in particular glacier flow; i.e. rates of tens to hundreds of metres per year; Figure 6), can be quantified also from medium-resolution satellite imagery (e.g. Landsat ETM+, ASTER) (30,39,49,53,54).

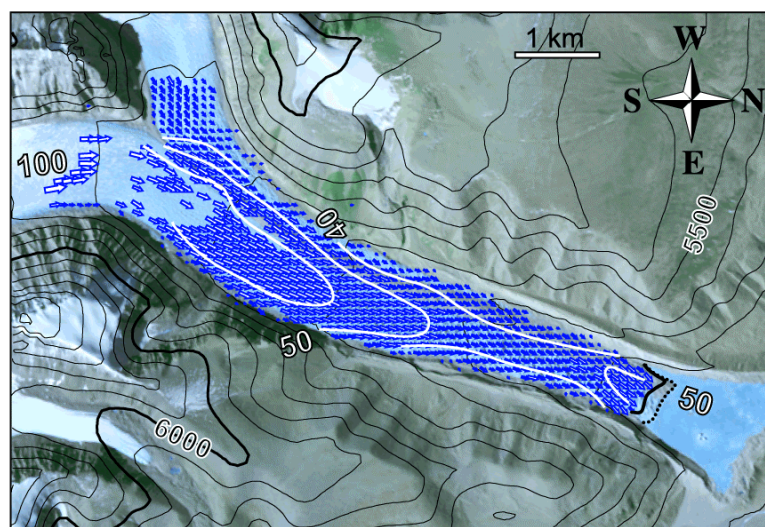


Figure 6: Horizontal surface velocities on a glacier (name unpublished) at the northern slope of the Bhutan Himalaya towards the Tibet plateau, derived from ASTER data of 20/01/2001 and 20/11/2001. Speed isolines are in m per year. Contour lines are in m a.s.l. and derived from the SRTM DTM. The dotted line at the calving front marks its position in 01/2001; the bold line is the 11/2001 position.

DETECTION OF HAZARD SOURCES

Detection of potential hazard sources is an important first step in assessing glacial risks. According to the nature of high-mountain processes, multidomain (or multidimensional) classification approaches that integrate spatial, spectral and temporal information are most promising for that task. No detailed rules for such multidomain classifications can be given due to the variety of specific requirements. In general, however, the combination of a DTM with multispectral and possibly multitemporal data is a particularly powerful tool for detecting potential high-mountain hazard sources. Selected examples include:

- Hanging glaciers, a source of ice break-offs and ice avalanches, can be detected on a regional scale through the combination of a multispectral glacier classification with the DTM slope. The result is a map of steep glaciers, i.e. above a certain slope threshold (Figure 7). According to empirical investigations in the Swiss Alps cold glaciers produce ice avalanches from a minimum bed slope of 45 degree, temperate glaciers from 25 degree (20).
- A texture analysis based on high-resolution satellite (or aerial) imagery combined with DTM slope helps to detect steep debris slopes prone to debris flow initiation (13).

- Glacier slope, extent of debris cover, thickness changes and ice velocities can help to estimate the evolution of ice-marginal lakes or detecting glacier zones prone to the development of supraglacial lakes (Figure 8) (30,55).
- Glacier length changes, possibly resulting in a change in ice-avalanche hazard or in proglacial lakes, can be tracked from multi-temporal and -spectral classification (23,55,56).
- Similarly, the (change in) ice cover on glacier-clad volcanoes, as detected from (repeat) multi-spectral imagery, can be an important factor for devastating lahars, in particular in connection with volcanic activity (57,58).
- Freshly deglaciaded sections (detectable by multi-temporal and -spectral classification) of rock walls (detectable by DTM slope and possibly texture analysis) indicate zones of potentially enhanced rockfall activity due to the thermal, mechanical and hydrological consequences accompanying glacier retreat (59).

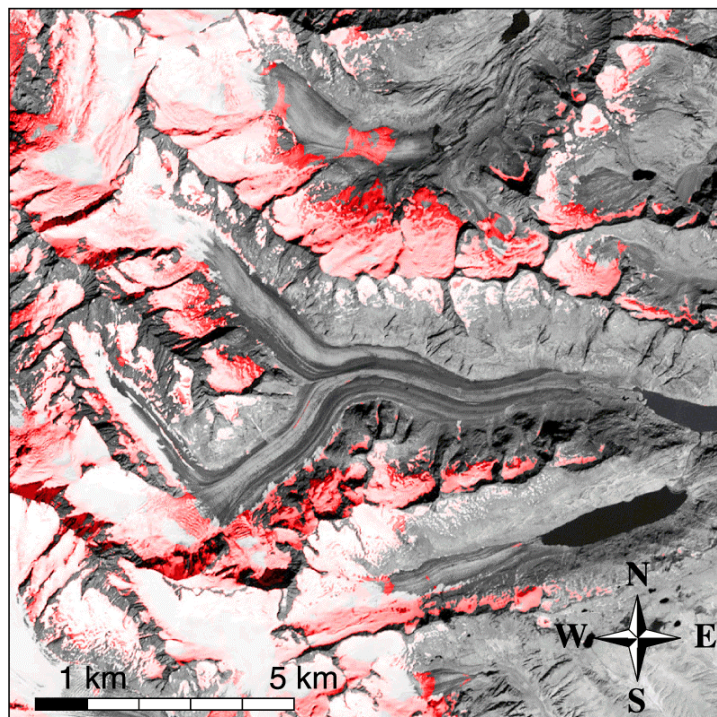


Figure 7: Steep glaciers as determined by a combination of a thresholded ASTER band 3 / ASTER band 4 ratio-image and a thresholded slope map with slope greater than 30 degree. The resulting image was coloured red and the intensity component fused from ASTER band 3.

A second class of multidomain classifications utilises not only the remotely sensed data itself, but also the outputs from process models, which might in turn be fed by remote sensing data. For instance, mountain permafrost distribution is highly dependent on elevation (as a surrogate for air temperature) and direct incoming solar radiation (60). Both can be derived from a DTM (61). As a second example, potentially debris-producing rock walls can be approximated as steep DTM sections without vegetation (from multispectral classification). Rockfall modelled from such terrain sections can then support remote sensing-based debris detection (62).

HAZARD POTENTIALS AND DISASTER MANAGEMENT

Once potential hazard sources have been detected, mass movement models help estimating potentially affected zones (13,19,20,63,64,65,66,67). The most important prerequisite of such models is a DTM, best obtained from remote sensing. This relates to the importance of topography for controlling mass-movement downslope propagation. Further, remote sensing supports mass movement modelling by providing model inputs through image classification such as surface cover, surface roughness, material to be potentially mobilised, etc. In addition, potentially endangered areas

can be investigated, possible chain reactions and secondary effects assessed, and settlements and infrastructure at risk can be mapped using remote sensing methods.

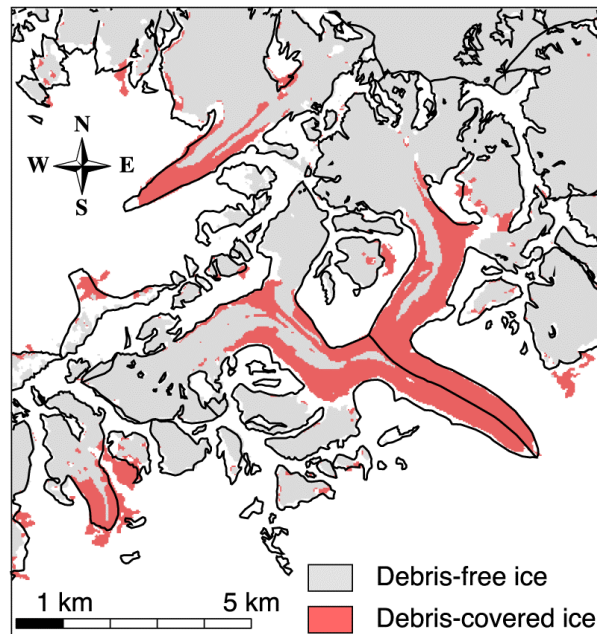


Figure 8: Automatic mapping of debris-covered ice from merging spectral data and DTM-slope. Areas that (i) have a slope < 23 degree, (ii) are not vegetated according to the normalized difference vegetation index (NDVI), and (iii) are in direct contact with debris-free ice as mapped from a thresholded ratio-image (Landsat TM band 4 / Landsat TM band 5) are classified as debris-covered ice (68). The black glacier outlines are taken from the 1973 Swiss glacier inventory (69).

The above paragraph relates to hazards, i.e. potential processes, the following paragraph to actions after a catastrophic event. Integrating remote sensing in the management of glacier- and permafrost-related disasters can serve three major applied and scientific needs: (i) overview of disaster and damage extent, (ii) frequent monitoring, and (iii) documentation. (i) and (ii) are directed towards search and rescue operations, and civil protection, and require a rapid and repeat data acquisition and processing. The short repeat cycle of satellite imagery (in urgent cases about two days, e.g. for ASTER) make spaceborne methods highly suitable for disaster management (12). Due to the limitations of optical remote sensing during cloud cover and night time, the application of (repeat) weather- and sun-independent SAR data can be especially important (70). The major problems related to (i) and (ii) are the end user capacity to handle and analyse the data, and the speed of data acquisition and delivery. Remotely sensed documentation of a disaster (iii), even if the data are not analysed immediately, can be a unique source for thoroughly investigating the processes involved, and for drawing scientific and applied conclusions of broader interest (e.g. (26)). Documentation of disaster extent and damages are further of interest for damage assessment and insurance purposes.

The International Charter „Space and Major Disasters“ offers potentially important remote-sensing support for managing large glacier and permafrost disasters. Within this contract, a number of space agencies and commercial satellite companies provide rapid and free emergency imaging under certain circumstances. Currently available sensors include ENVISAT, ERS, IRS, Radarsat, or SPOT. Only selected national and international civil protection, rescue and security authorities can activate the [Charter](#). Also, the ASTER sensor onboard TERRA can be activated for supporting disaster management (12).

CONCLUSIONS AND PERSPECTIVES

Due to the challenges, with which hazard experts and responsible authorities in mountains are presently faced, on the one hand, and due to the current development in air- and space-

technology, on the other hand, remote sensing is becoming an increasingly important and integrative component of glacier and permafrost hazard assessment and management. Spaceborne remote sensing offers support for assessing the hazard disposition (i.e. the hazard potential), rather than enabling the observation of trigger conditions and, thus, the direct short-term forecast of events.

A major factor limiting the accuracy and applicability of methods based on spaceborne sensors is their spatial resolution. However, data from high-resolution sensors such as IKONOS, QuickBird or Orbview3 open new possibilities for glacier and permafrost hazard assessment in this respect, but are still very expensive and only able to cover small areas (Figure 9) (13,26,36,50,71).

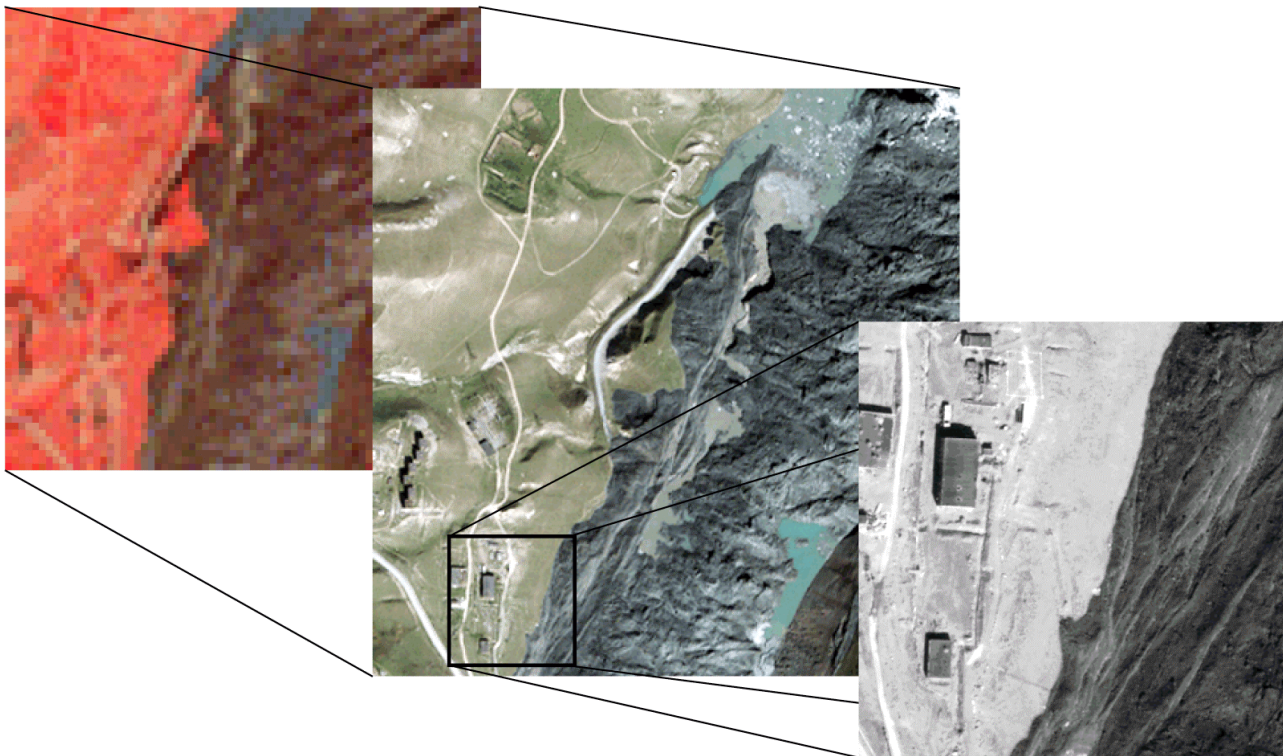


Figure 9: Rock-ice avalanche deposits at Karmadon as seen from ASTER (15 m resolution; left), QuickBird multispectral (2.5 m resolution; middle) and QuickBird panchromatic (0.6 m resolution; right). QuickBird data © Digitalglobe.

Modern space technologies enable initial estimation of hazard potentials to be performed by virtually everyone and everywhere, independent of political and geographical restrictions. This fundamental "democratisation" process related to high-mountain (and other) hazards involves a number of new opportunities, dangers and responsibilities for the public, the authorities in charge, and the experts involved. Hazard assessment based on spaceborne remote sensing has, therefore, to follow certain rules considering these responsibilities and the consequences of their disregard. Corresponding recommendations are presently compiled by the international working group on glacier and permafrost hazards in mountains by the Commission on Cryospheric Sciences (CCS) and the International Permafrost Association (IPA).

ACKNOWLEDGEMENTS

The ASTER scenes used in the presented studies were provided within the framework of the Global Land Ice Measurements from Space project (GLIMS) through the EROS data center, and by courtesy of NASA/GSFC/METI/ERSDAC/JAROS, and the US/Japan ASTER science team. Some of the studies were conducted for, or in close co-operation with, the Swiss Agency for Development and Co-operation (SDC).

REFERENCES

- 1 Kääb A, J M Reynolds & W Haeberli, 2005. Glacier and permafrost hazards in high mountains. In: Global Change and Mountain Regions (A State of Knowledge Overview), edited by U M Huber, H K M Bugmann & M A Reasoner (Springer, Dordrecht), 225-234
- 2 Sabins F F, 1997. Remote sensing: principles and interpretation. (Freeman)
- 3 Ostir K, T Veljanovski, T Podobnikar & Z Stancic, 2003. Application of satellite remote sensing in natural hazard management: the Mount Mangart landslide case study. International Journal of Remote Sensing, 24(20): 3983-4002
- 4 Kääb A, 2004. Mountain glaciers and permafrost creep. Methodical research perspectives from earth observation and geoinformatics technologies. Habilitation thesis, Department of Geography, University of Zurich, 205 pp.
- 5 Huggel C, 2004. Assessment of glacial hazards based on remote sensing and GIS modeling, Department of Geography, University of Zurich, Physical Geography Series, 44
- 6 Quincey D, R M Lucas, S D Richardson, N F Glasser, M J Hambrey & J M Reynolds, 2005. Optical remote sensing techniques in high-mountain environments: application to glacial hazards. Progress in Physical Geography: in press.
- 7 Gao J & Y S Liu, 2001. Applications of remote sensing, GIS and GPS in glaciology: a review. Progress in Physical Geography, 25(4): 520-540
- 8 Buchroithner M F, G Jentsch & B Waniverhaus, 1982. Monitoring of recent glaciological events in the Khumbu Area (Himalaya, Nepal) by digital processing of Landsat MSS data. Rock Mechanics, 15(4): 181-197
- 9 Kääb A, W Haeberli, C Huggel & F Paul, 2000. Glacier- and permafrost-related hazards in high mountains: integrative assessment in the Swiss Alps based on remote sensing and geo-information systems. In X Congresso Peruano de Geologia, CD-ROM
- 10 Huggel C, A Kääb, W Haeberli, P Teysseire & F Paul, 2002. Satellite and aerial imagery for analysing high mountain lake hazards. Canadian Geotechnical Journal, 39(2): 316-330
- 11 Silverio W & J-M Jaquet, 2005. Glacial cover mapping (1987-1996) of the Cordillera Blanca (Peru) using satellite imagery. Remote Sensing of Environment, 95: 342-350
- 12 Kääb A, R Wessels, W Haeberli, C Huggel, J Kargel & S J S Khalsa, 2003. Rapid ASTER imaging facilitates timely assessment of glacier hazards and disasters. EOS Transactions, American Geophysical Union, 84(13): 117-121
- 13 Huggel C, A Kääb & N Salzmann, 2004. GIS-based modeling of glacial hazards and their interactions using Landsat TM and Ikonos imagery. Norwegian Journal of Geography, 58: 61-73
- 14 Liu J G, P J Mason, N Clerici, S Chen, A Davis, F Miao, H Deng & L Liang, 2005. Landslide hazard assessment in the Three Gorges area of the Yangtze river using ASTER imagery: Zigui-Badong. Geomorphology, 61(1-2): 171-187
- 15 Toutin T, 2001. DEM generation from new VIR Sensors: Ikonos, ASTER and Landsat 7. In: Proceedings Geoscience and Remote Sensing Symposium, 2001. IGARSS'01. IEEE 2001 International, 3, 973-975
- 16 Gamache M, 2004. Free and Low Cost Datasets for International Mountain Cartography. In 4th ICA Mountain Cartography Workshop
- 17 Hall D, A T C Chang, J L Foster, C S Benson & W M Kovalick, 1989. Comparison of in situ and Landsat derived reflectances of Alaskan glaciers. Remote Sensing of Environment, 28: 493-504

- 18 Paul F, A Käab, M Maisch, T Kellenberger & W Haeberli, 2004. Rapid disintegration of Alpine glaciers observed with satellite data. Geophysical Research Letters: L21402, doi:10.1029/2004GL020816
- 19 Käab A, C Huggel, F Paul, R Wessels, B Raup, H Kieffer & J Kargel, 2003. Glacier monitoring from ASTER imagery: accuracy and applications. EARSeL eProceedings, 2: 43-53
- 20 Salzmann N, A Käab, C Huggel, B Algöwer & W Haeberli, 2004. Assessment of the hazard potential of ice avalanches using remote sensing and GIS-modelling. Norwegian Journal of Geography, 58: 74-84
- 21 Paul F, A Käab, M Maisch, T Kellenberger & W Haeberli, 2002. The new remote-sensing-derived Swiss glacier inventory: I. Methods. Annals of Glaciology, 34: 355-361
- 22 Aniya M, H Sato, R Naruse, P Skvarca & G Casassa, 1996. The use of satellite and airborne imagery to inventory outlet glaciers of the Southern Patagonia Icefield, South America. Photogrammetric Engineering and Remote Sensing, 62: 1361-1369
- 23 Albert T, 2002. Evaluation of remote sensing techniques for ice-area classification applied to the tropical Quelccaya ice cap, Peru. Polar Geography, 26(3): 210-226
- 24 Wessels R, J S Kargel & H H Kieffer, 2002. ASTER measurement of supraglacial lakes in the Mount Everest region of the Himalaya. Annals of Glaciology, 34: 399-408
- 25 Haeberli W, C Huggel, A Käab, S Oswald, A Polvoj, I Zotikov & N Osokin, 2005. The Kolka-Karmadon rock/ice slide of 20 September 2002 - an extraordinary event of historical dimensions in North Ossetia (Russian Caucasus). Journal of Glaciology: in press
- 26 Huggel C, S Zraggen-Oswald, W Haeberli, A Käab, A Polkvoj, I Galushkin & S G Evans, 2005. The 2002 rock/ice avalanche at Kolka/Karmadon, Russian Caucasus: assessment of extraordinary avalanche formation and mobility, and application of QuickBird satellite imagery. Natural Hazards and Earth System Sciences, 5: 173-187
- 27 Kotlyakov V M, O V Rototaeva & G A Nosenko, 2004. The September 2002 Kolka glacier catastrophe in North Ossetia, Russian Federation. evidence and analysis. Mountain Research and Development, 2(1): 78-83
- 28 Schowengerdt, 1997. Remote sensing. Models and methods for image processing - second edition (Academic Press)
- 29 Käab A, Y Isakowski, F Paul, A Neumann & R Winter, 2003. Glaziale und periglaziale Prozesse: Von der statischen zur dynamischen Visualisierung. Kartographische Nachrichten, 53(5): 206-212
- 30 Käab A, 2005. Combination of SRTM3 and repeat ASTER data for deriving alpine glacier flow velocities in the Bhutan Himalaya. Remote Sensing of Environment, 94(4): 463-474
- 31 Rott H & D Strobl, 1992. Synergism of SAR and Landsat TM imagery for thematic mapping in complex terrain. Advances in Space Research, 12(7): 425-431
- 32 Rott H, 1994. Thematic studies in alpine areas by means of polarimetric SAR and optical imagery. Advances in Space Research, 14(3): 217-226
- 33 König M, J-G Winther & E Isaksson, 2001. Measuring snow and ice properties from satellite. Reviews of Geophysics, 39(1): 1-27
- 34 Toutin T, 2002. Three-dimensional topographic mapping with ASTER stereo data in rugged topography. IEEE Transactions on Geoscience and Remote Sensing, 40(10): 2241-2247
- 35 Hirano A, R Welch & H Lang, 2003. Mapping from ASTER stereo image data: DEM validation and accuracy assessment. ISPRS Journal of Photogrammetry and Remote Sensing, 57(5-6): 356-370

- 36 Berthier E, Y Arnaud, D Baratoux, C Vincent & F Remy, 2004. Recent rapid thinning of the 'Mer de Glace' glacier derived from satellite optical images. Geophysical Research Letters, 31: L17401, doi:10.1029/2004GL020706
- 37 Stevens N F, H Garbeil & P J Mouginis-Mark, 2004. NASA EOS Terra ASTER: Volcanic topographic mapping and capability. Remote Sensing of Environment, 90: 405-414
- 38 Zollinger S, 2003. ASTER satellite data for automatic generation of DEMs in high mountains. Mt. Everest region. Diploma thesis (Department of Geography, Library, University of Zurich) 172 pp.
- 39 Käab A, B Lefauconnier & K Melvold, 2004. Flow field of Kronebreen, Svalbard, using repeated Landsat7 and ASTER data. Annals of Glaciology, 42: in press
- 40 Weidmann Y, 2004. Kombination von ASTER- und SRTM-Höhenmodellen für die Abschätzung von Naturgefahren im Pamir Gebirge, Tadschikistan. Diploma thesis (University of Applied Sciences, Muttenz, Basel) 40 pp.
- 41 Baltsavias E P, 1996. Digital ortho-images – a powerful tool for the extraction of spatial- and geo-information. ISPRS Journal of Photogrammetry and Remote Sensing, 51(2): 63-77
- 42 Schmutz K, 2005. ASTER- und SRTM-basierte Fernerkundung der Kolka-Karmadon Fels-/Eislawine in Nordossetien, Russischer Kaukasus. Diploma thesis (Department of Geography, University of Zurich) in press
- 43 Honikel M, 2002. Fusion of spaceborne stereo-optical and interferometric SAR data for digital terrain model generation, Mitteilungen des Institutes für Geodäsie und Photogrammetrie, 76
- 44 Käab A, 1996. Photogrammetrische Analyse zur Früherkennung gletscher- und permafrostbedingter Naturgefahren im Hochgebirge, Mitteilungen der Versuchsanstalt für Wasserbau, Hydrologie und Glaziologie der ETH Zürich, 145, 182 pp.
- 45 Käab A, 2000. Photogrammetry for early recognition of high mountain hazards: new techniques and applications. Physics and Chemistry of the Earth, Part B, 25(9): 765-770.
- 46 Käab A & M Vollmer, 2000. Surface geometry, thickness changes and flow fields on creeping mountain permafrost: automatic extraction by digital image analysis. Permafrost and Periglacial Processes, 11(4): 315-326
- 47 Käab A, W Haerberli & G H Gudmundsson, 1997. Analysing the creep of mountain permafrost using high precision aerial photogrammetry: 25 years of monitoring Gruben rock glacier, Swiss Alps. Permafrost and Periglacial Processes, 8(4): 409-426
- 48 Gudmundsson G H & A Bauder, 1999. Towards an indirect determination of the mass-balance distribution of glaciers using the kinematic boundary condition. Geografiska Annaler, 81A(4): 575-583
- 49 Käab A, 2002. Monitoring high-mountain terrain deformation from air- and spaceborne optical data: examples using digital aerial imagery and ASTER data. ISPRS Journal of Photogrammetry and Remote Sensing, 57(1-2): 39-52
- 50 Delacourt C, P Allemand, B Casson & H Vadon, 2004. Velocity field of "La Clapière" landslide measured by the correlation of aerial and QuickBird satellite images. Geophysical Research Letters, 31(15), L15619, doi:10.1029/2004GL020193
- 51 Strozzi T, A Luckman, T Murray, U Wegmüller & C L Werner, 2002. Glacier motion estimation using SAR offset-tracking procedures. IEEE Transactions on Geosciences and Remote Sensing, 40(11): 2384-2391
- 52 Michel R & E Rignot, 1999. Flow of Moreno Glacier, Argentina, from repeat-pass Shuttle Imaging Radar images: comparison of the phase correlation method with radar interferometry. Journal of Glaciology, 45(149): 93-100

- 53 Skvarca P, B Raup & H De Angelis, 2003. Recent behaviour of Glaciar Upsala, a fast-flowing calving glacier in Lago Argentino, southern Patagonia. Annals of Glaciology, 36: 184-188
- 54 Dowdeswell J A & T J Benham, 2003. A surge of Perseibreen, Svalbard, examined using aerial photography and ASTER high-resolution satellite imagery. Polar Research, 22(2): 373-383
- 55 Paul F, C Huggel & A Kääb, 2004. Mapping of debris-covered glaciers using multispectral and DEM classification techniques. Remote Sensing of Environment, 89(4): 510-518
- 56 Paul F, 2001. Evaluation of different methods for glacier mapping using Landsat TM. EARSeL eProceedings, 1: 239-245
- 57 Major J J & C G Newhall, 1989. Snow and ice perturbation during historical volcanic eruptions and the formation of lahars and floods. Bulletin of Volcanology, 52: 1-27
- 58 Thouret J C, 1990. Effects of the November 13, 1985 eruption on the snow pack and ice cap of Nevado del Ruiz volcano, Colombia. Journal of Volcanology and Geothermal Research, 41: 177-201
- 59 Fischer L, 2004. Monte Rosa Ostwand - Geologie, Vergletscherung, Permafrost und Sturzergebnisse in einer hochalpinen Steilwand. Diploma thesis (Departments of Earth Sciences, ETH Zurich, and Geography, [Library](#), University of Zurich) 104 pp.
- 60 Hoelzle M, 1992. Permafrost occurrence from BTS measurements and climatic parameters in the eastern Swiss Alps. Permafrost and Periglacial Processes, 3(2): 143-147
- 61 Hoelzle M, 1996. Mapping and modelling of mountain permafrost distribution in the Alps. Norwegian Journal of Geography, 50: 11-15
- 62 Stumm D, 2001. Erkennung geomorphologischer Formen mit Hilfe von GIS und Fernerkundung. Diploma thesis (Department of Geography, [Library](#), University of Zurich) 72 pp.
- 63 Huggel C, A Kääb, W Haeberli & B Krummenacher, 2003. Regional-scale GIS-models for assessment of hazards from glacier lake outbursts: evaluation and application in the Swiss Alps. Natural Hazards and Earth System Science, 3(6): 647-662
- 64 Schlaefli S, 2005. Interaktive, GIS-basierte Modellierung von Murgängen, Fels- und Eislawinen. Diploma thesis (Department of Geography, [Library](#), University of Zurich) 71 pp.
- 65 Noetzli J, C Huggel, M Hoelzle & W Haeberli, 2005. GIS-based modelling of rock/ice avalanches from Alpine permafrost areas. Computational Geosciences: in press
- 66 Stevens N F, V Manville & D W Heron, 2003. The sensitivity of a volcanic flow model to digital elevation model accuracy: experiments with digitised map contours and interferometric SAR at Ruapehu and Taranaki volcanoes, New Zealand. Journal of Volcanology and Geothermal Research, 119(1-4): 89-105
- 67 Iverson R M, S P Schilling & J W Vallance, 1998. Objective delineation of lahar-inundation hazard zones. Geological Society of America Bulletin, 110(8): 972-984
- 68 Paul F, 2004. The new Swiss glacier inventory 2000 – Application of remote sensing and GIS. PhD thesis (Department of Geography, University of Zurich) 189 pp.
- 69 Maisch M, A Wipf, B Denneler, J Battaglia & C Benz, 1999. Die Gletscher der Schweizer Alpen: Gletscherhochstand 1850 - Aktuelle Vergletscherung - Gletscherschwund-Szenarien 21. Jahrhundert. (vdf Hochschulverlag, ETH Zurich), Schlussbericht NFP31
- 70 Kerle N & C Oppenheimer, 2002. Satellite remote sensing as a tool in lahar disaster management. Disasters, 26(2): 140-160
- 71 Huggel C, A Kääb & N Salzmann, 2005. Evaluation of QuickBird and IKONOS imagery for assessment of high-mountain hazards. Submitted to EARSeL eProceedings